

Miniaturized Robotic End-Effector With Piezoelectric Actuation and Fiber Optic Sensing for Minimally Invasive Cardiac Procedures

Edgar Aranda-Michel, Jaehyun Yi, Jackson Wirekoh, Nitish Kumar, *Member, IEEE*,
Cameron N. Riviere[✉], *Senior Member, IEEE*, David S. Schwartzman, and Yong-Lae Park[✉], *Member, IEEE*

Abstract—Each year 35 000 cardiac ablation procedures are performed to treat atrial fibrillation through the use of catheter systems. The success rate of this treatment is highly dependent on the force which the catheter applies on the heart wall. If the magnitude of the applied force is much higher than a certain threshold the tissue perforates, whereas if the force is lower than this threshold the lesion size may be too large and is inconsistent. Furthermore, studies have shown large variability in the applied force from trained physicians during treatment, suggesting that although there might be patient-specific differences, physicians are unable to manually regulate the levels of the force at the site of treatment. Current catheter systems do not provide the physicians with active means for contact force control and are only at most aided by visual feedback of the forces measured *in situ*. This paper discusses a novel design of a robotic end-effector that integrates mechanisms of sensing and actively controlling of the applied forces into a miniaturized compact form. The required specifications for design and integration were derived from the current application under investigation. An off-the-shelf miniature piezoelectric motor was chosen for actuation, and a force sensing solution was developed to meet the specifications. Experimental characterization of the actuator and the force sensor within the integrated setup show compliance with the specifications and pave the way for future experimentation where closed-loop control of the system can be implemented according to the contact force control strategies for the application.

Index Terms—Force sensing, piezoelectric actuator, fiber Bragg gratings (FBGs), functionalized catheter tip, cardiac ablation, atrial fibrillation, minimally invasive procedures.

Manuscript received January 26, 2018; revised March 28, 2018; accepted March 28, 2018. Date of publication April 20, 2018; date of current version May 22, 2018. This work was supported by the National Heart, Lung, and Blood Institute, National Institutes of Health, under Grant R21HL126081. The associate editor coordinating the review of this paper and approving it for publication was Prof. Subhas C. Mukhopadhyay. (*Corresponding author: Yong-Lae Park.*)

E. Aranda-Michel is with the Medical Scientist Program, University of Pittsburgh, Pittsburgh, PA 15260 USA, and Carnegie Mellon University, Pittsburgh, PA 15261 USA.

J. Yi is with the Department of Mechanical and Aerospace Engineering, Seoul National University, Seoul 08826, South Korea.

J. Wirekoh, N. Kumar, and C. N. Riviere are with the Robotics Institute, Carnegie Mellon University, Pittsburgh, PA 15213 USA.

D. S. Schwartzman is with the Cardiology Department, Butler Health System (BHS), Butler, PA 16001 USA.

Y.-L. Park is with the Department of Mechanical and Aerospace Engineering and the Institute of Advanced Machines and Design, Seoul National University, Seoul 08826, South Korea, and also with the Robotics Institute, Carnegie Mellon University, Pittsburgh, PA 15213 USA (e-mail: ylpark@snu.ac.kr).

Digital Object Identifier 10.1109/JSEN.2018.2828940

I. INTRODUCTION

MINIMALLY invasive surgery (MIS) is a rising trend in medicine, having been adopted into nearly every medical field [1], [2]. The growth in the type of MIS surgeries can largely be attributed to its numerous advantages, which include shorter recovery times, decreases in complication rates, and increases in the functional results of the procedures [3]–[6]. To successfully perform these procedures, catheters are equipped with functionalized tips capable of sensing, actuation, and/or the application of treatment as in ablation procedures. During these treatments, which are increasingly being performed in the U.S. [7], abnormally functioning cells are destroyed. Of these procedures, a large portion (30 000–35 000) is cardiac ablation procedures, which are used to treat atrial fibrillation (AF) through two main methods of ablation: radio frequency ablation (RFA) and cryogenic ablation. During both of these procedures, the applied force of the catheter tip on the abnormal cell tissue is critical to the success of the treatment. In RFA, the applied force determines how much energy is transferred to the tissue and thus the lesion size [8]–[11], while in cryogenic ablation the force is critical to the formation of the lesion as well [12]. The efficacy and safety of catheter ablation of AF has been surveyed, reporting a success rate (i.e. freedom from symptomatic AF in the absence of antiarrhythmic therapy) of 52%, with 6% major complications [13].

During the AF treatment, the physician pushes on one end of a long flexible catheter in a sheath to apply force to the treatment site. Investigations into force application by this method revealed large variations in applied forces [14]–[16]. Several advancements in catheter technology have aimed at resolving this issue by designing catheters capable of measuring the applied force at the tip [17], [18] and providing a visual feedback. The visual feedback, though useful, may not be sufficient in many cases as the physician's response time might vary leading to inconsistent force applications. Moreover, these catheter systems do not provide any haptic force feedback either to the physicians to improve his/her reaction. To mitigate the lack of haptic force feedback, efforts have been made to equip the catheters with external actuation [19], [20] to control the applied forces. This kind of external actuation is motivated by the geometric constraints of the veins with which

the catheters and their sheaths must traverse to reach the heart. Commercially available catheter sheaths, designed to provide navigation for the catheters to the site of treatment, restrict the external diameter of ablation catheters to 3 mm, which makes the integration of actuation and sensing very difficult at the catheter tip. However, this indirect method of actuating the catheter inside the sheath from outside the body suffers from its own complications. In particular, the modeling of the system being controlled becomes increasingly complex due to presence of friction caused by random contacts between the sheath and catheter, and viscous forces caused by the motion between the catheter and the sheath in vivo. In this workflow, where the actuation is external to the catheter, the physician also loses control over the catheter inside the sheath and over the procedure. This study provides an alternative perspective to the problem of integrating sensing and actuation in the functionalized catheter tip for the treatment of AF, proposing the design of a miniaturized tip integrating actuation and sensing which can be embedded at the tip of conventional catheters. The advantage of this approach lies in the in situ actuation of the catheter tip, as opposed to external actuation, which makes the system modeling and force control more transparent and straightforward. Moreover, such a design keeps the manual control of the catheter still in the hands of the physician, which is desirable for safety.

This paper discusses a novel design of a robotic end-effector that integrates the sensing of the applied forces with an active means of controlling them into a miniaturized compact form. First, the required specifications for such a design and integration were derived from the current application under investigation. An off-the-shelf miniaturized piezoelectric motor was chosen for the actuation and a uniaxial force sensing solution was developed according to the required specifications. Experimental characterization of the actuator and the force sensor within the integrated setup show compliance with the developed specifications and pave the way for future experimentation where closed loop control of the integrated system can be implemented according to the contact force control strategies needed for the application.

The remainder of this study is divided into three sections. Section II develops the specifications for the design of the miniaturized catheter tip for the treatment of AF. It also details the design and fabrication of the functionalized tip and how the compact integration of actuation and sensing was achieved. Section III discusses the experimental characterization of the actuation and sensing units individually and within the integrated setup, thereby validating the design against the specifications developed earlier. Section IV provides the conclusion and perspectives for the current work.

II. DESIGN AND FABRICATION

The key requirement specifications that guide the design and integration of the needed actuation and sensing are listed. These specifications are derived from the specific application case of AF treatment via catheter ablation. Subsequently, the design and fabrication of the miniaturized tip is detailed.

A. Specifications

1) *Size*: The AF treatment begins with first placing the catheter sheath inside the blood vessel through which a catheter is later inserted. The size of the blood vessel determines the diameter of the catheter sheath and in turn of the catheter used for the treatment, which ranges from 6-15 Fr (2–4.5 mm) [16].

2) *Actuation*: In this study, we aim to develop a robotic catheter tip where actuation is local and internal, rather than effected by means external to the catheter. Apart from the constraints on the size, the designed or chosen actuator must be able to apply a force in the range of 0–0.5N [17], which is observed during diverse catheter ablation procedures. Since the catheter tip should remain in touch with the heart wall during the procedure, limits on the linear displacement and the linear speed of the actuator should be enough to compensate for the heart wall movement caused due to the beating of the heart and expansion/contractions of the lungs during breathing.

3) *Force Sensing*: At minimum, one degree of freedom (DOF) in the force sensing is required to measure the interaction force between the tip and heart tissue. The force sensor should be able to measure a maximum force of 0.5 N, which is same as required for the actuation. An in-depth requirements list for the force sensing for catheter ablation procedures can be found in [17].

B. Actuation and Sensing

The piezoelectric linear motor (SQL-RV-1.8, Squiggle Micro Motor, New Scale Technologies), which has been used in controlling a micro device [21] and micromanipulation [22], has been selected for the actuation. This motor has a $2.8 \times 2.8 \text{ mm}^2$ cross-sectional area with a 6 mm length as well as force output up to 50 g (0.49 N). Thus it is compact enough for the catheter ablation procedures while being able to provide sufficient force output.

Previously described fiber optic sensing using fiber Bragg gratings (FBGs) to detect tip force [23]–[25] and deflection [26], [27] of end-effectors for robotic and MIS applications was chosen for the force sensing. Axial force can be optically detected by measuring reflection wavelength shifts that are proportional to mechanical strain changes on the FBG area within a specific region of the fiber. The sensitivity of the FBG to applied forces, in addition to its small size, made it ideal for integration with our miniature piezoelectric motor into the final tip design.

C. Design of Integrated Setup and Fabrication

Fig. 1 shows the integral elements of the design, incorporating both actuation and sensing components. The piezoelectric motor applies a helical twist to the housing causing it to rotate around the screw and move it forwards or backwards. Therefore the tip is not attached, but kept in constant contact with the screw through the use of an extension spring. The spring, which has a stiffness of 35 N/m, was chosen to fit the necessary physical profile of the catheter while allowing full range of motion of the tip. In designing the housing, consideration was given to the following: the alignment of the tip shaft with the screw, the restriction of off-axis movement

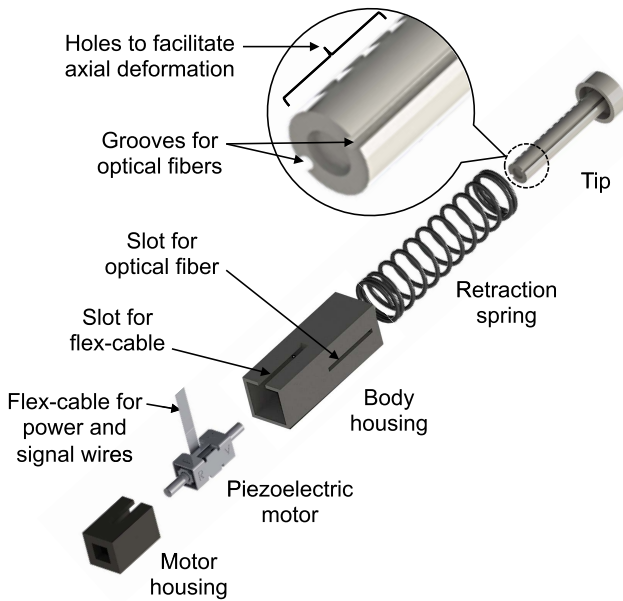


Fig. 1. Design of overall components of the robotic end-effector with an exploded view. The zoomed-in area shows the structure of the tip that contains grooves for embedding optical fibers and multiple holes in series to facilitate axial deformation for tip force sensing.

of the tip shaft, and the relative locking of the motor with the housing. The rationale for the first two design choices was due to the piezoelectric motor. Transverse forces applied to the screw shaft and thus the motor severely hinder the output of the motor.

To augment the device with the optical fiber for force sensing, two features were incorporated into the tip design. Firstly, grooves of 3.5 mm diameter are running along the longitudinal axis to house the fiber and to allow for permanent adhesion of the fiber to the tip. Secondly, to ensure the tip is flexible enough to deform, transmitting the force to the fiber as well as still being structurally sound, 0.5 mm diameter holes were added through the center of the tip's shaft perpendicular to the longitudinal axis. These features are illustrated in Fig. 1. A key consideration was that temperature greatly affects the force reading of the fiber, offsetting it. Therefore, two optical fibers were utilized. One fiber was attached to the entire length of the groove. During tip strain, the fiber will experience the same strain. Thus, this fiber measures both the applied force and the thermal offset. The second fiber is attached at only a single point along the groove so that when the tip undergoes strain this fiber remains stationary, resulting in a measurement solely of the thermal offset. Having a recording of each optical fiber will allow for a compensation for the thermal offset.

Fig. 2 shows the complete prototype with key components indicated. The three-dimensional (3D) models of the catheter tip were ordered from Proto Lab FineLine, a stereolithography fabrication service, using their watershed material at a resolution of 50 μm . FineLine was chosen for their high resolution and efficiency in producing parts with minimal residual support material, which clogs the motor and screw. The spring was a Templeman EBE-010-513-S. The device was constructed in a clean area in order to prevent the clogging of

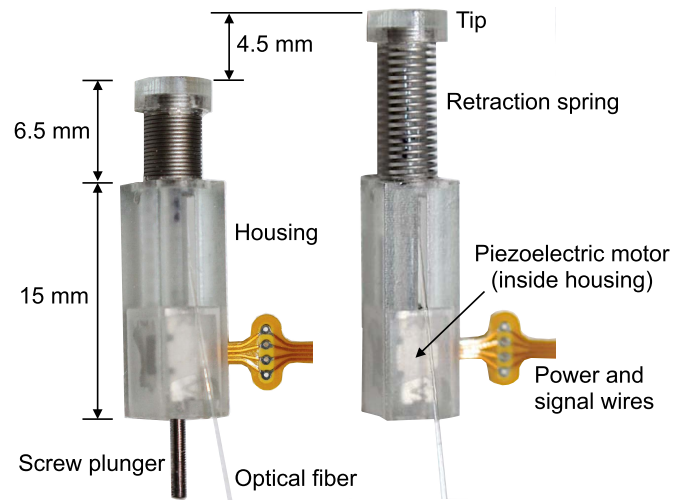


Fig. 2. Complete end-effector prototype before (left) and after (right) tip extension with linear piezoelectric motor.

the motor by ambient particulates. All parts were held together using cyanoacrylate glue with exception of parts 1 and 2, which are held together by a friction fit.

D. Safety

Another important requirement to be taken into account in the design stage is safety, since any defects in the system may cause a fatal condition of the patient during the procedure. The robotic end-effector we are proposing in this paper will be fully encased by a catheter sheath made of a biocompatible material, which will not only protect the soft tissue of the heart or blood vessels from any possible sharp corners of the end-effector, but also prevent blood inflow to the device, which may cause corrosion of metallic parts. The sheath also provides electrical insulation of the system and allows easy sterilization.

III. EXPERIMENTAL CHARACTERIZATION

To validate the tip design, it is necessary to evaluate the tip on the initial metrics that were set out. The primary requirements to be fulfilled are the tip speed, force output and the fiber-optic force sensing. The motor speed is designated by a duty cycle, which can be changed indirectly by changing the percentage of maximum speed, ranging from 10% to 100%.

A. Speed

A critical factor in validating the catheter tip was comparing the speed of the tip with the speed of the left atrium (LA) during systole, which is the site of ablation. The averaged data for both the forward and reverse motions are shown in Fig. 3 and Fig. 4. The tip speed of the forward motion tends to decrease gradually as the tip displacement increases. In contrast, the tip speed was relatively constant for the same duty cycle, rarely affected by the displacement. The difference of the tip speed between the forward and the reverse motions is due to the retraction spring located between the tip and the housing. The spring continuously exerts the retraction force to the tip and weakens the pushing force as the tip travels

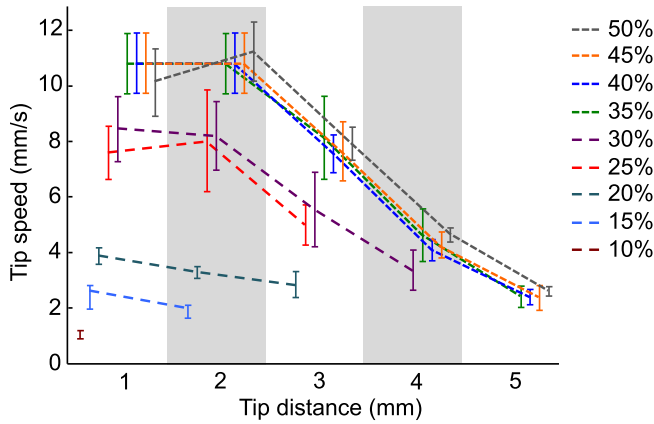


Fig. 3. Forward tip speed recorded at different tip distances and different percentages of maximum speed. The tip was laid on top of a ruler with the tip of the catheter positioned over the 0 mm marking. A DSLR camera recorded the motion of the tip at 60 fps. Five trials were done for each speed indicated. The speed was calculated over the step distance of 1 mm. All speeds are in the forward direction i.e. when the tip extends. The error bars show the standard deviation.

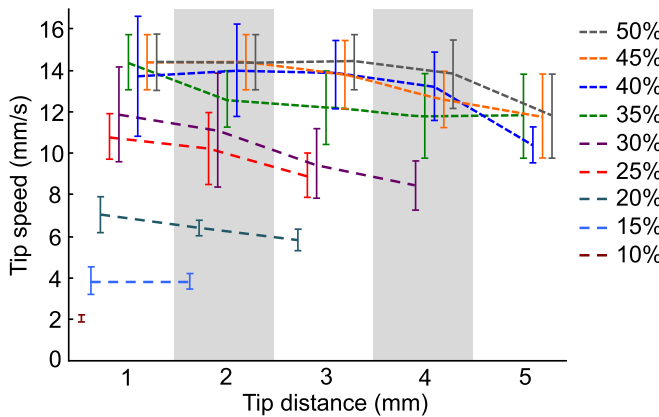


Fig. 4. Reverse tip speed recorded at different tip distances and different percentages of maximum speed. Five trials were done for each speed indicated. All speeds are in the reverse direction when the tip contracts. The error bars show the standard deviation.

longer, since the spring force increases as the displacement increases, which lead to gradual speed reduction during the forward motion. On the other hand, the spring does not reduce the force of the motor during the reverse motion, and the motor can maintain the tip speed relatively constant. The procedure involves creating scar tissue around the entry sites of the four pulmonary veins into the LA. These four sites are adhered to the posterior wall of the pleural space by attachments called pleural reflections. These attachments to the back of the chest cavity restrict the movement of this section of the LA during the cardiac cycle. As such, we expect the operating speed of the tip to be sufficient in accounting for any movement [28].

B. Force

The motor was tested at different percentages of the maximum speed. The values chosen ranged from 50% to 15%, stepping by 5% because any speed chosen above 50% showed no measurable change. In addition to the different speeds, different initial tip displacements were chosen. These values ranged from the initial tip position, 0 mm, to step below the

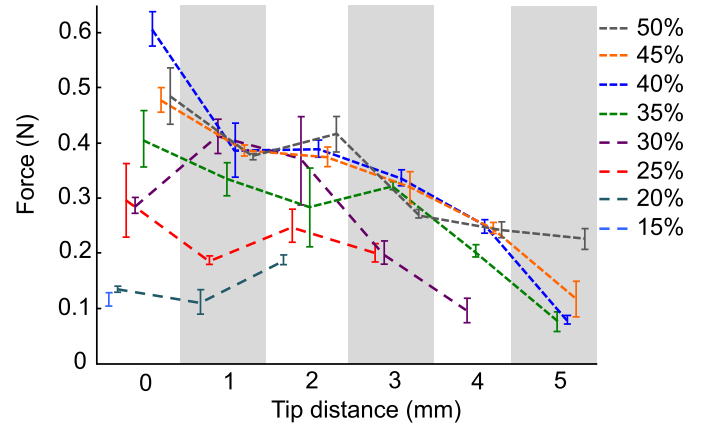


Fig. 5. Force data was plotted against the tip displacements and percentage of maximum speed. A commercial load cell was used to collect the data. The motor was fixed at the bottom of the test stand with clamps and the load cell was positioned at several different distances above the motor, indicated on the y-axis. For distances that do not have a force value the tip either could not make that distance or no force was detected.

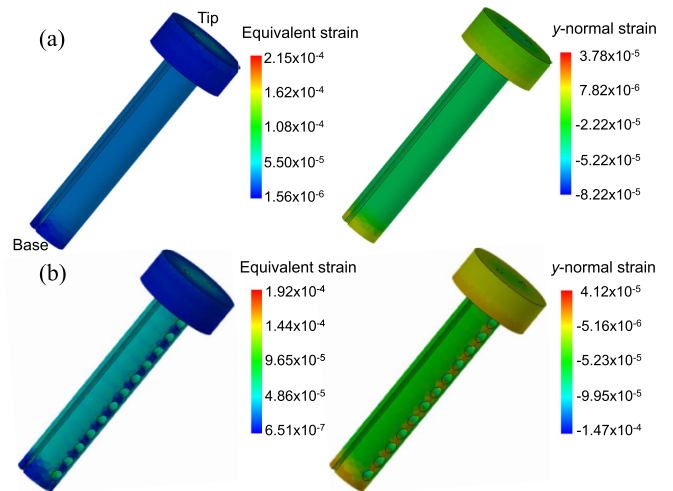


Fig. 6. (a) Equivalent strain distribution and (b) y -normal strain distribution when 1 N of axial force was applied to the top in normal direction while the base was fixed, which were simulated using SolidWorks.

maximum drive length of the motor, 5 mm. The displacements had a step size of 1 mm. The force for each test was recorded as the average steady state force after the initial decay. The data from each pairing was then averaged. Fig. 5 shows the result indicating gradual force reduction with tip displacement, similar to the trend of the forward tip speed. The average standard deviation of the force was about 10% of the average applied force. Of note is the horizontal red line, corresponding approximately to the minimum force level needed for the RF ablation procedures [17], [20]. The results show that the duty cycle needed to reach adequate force application is the one corresponding to maximum speed of 50%.

C. Force Sensing

First, a finite element analysis (FEA) was conducted to confirm the deformation of the catheter tip with an axial load using SolidWorks@Simulation. Fig. 6 shows the equivalent and y -normal strain of the tip. This step was to determine if

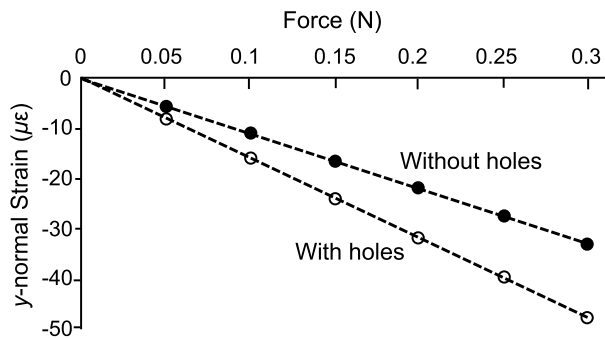


Fig. 7. Comparison of y -normal strains on the side-grooves of the tips without and with holes, respectively, up to 0.3 N of axial tip loading from FEA simulation.

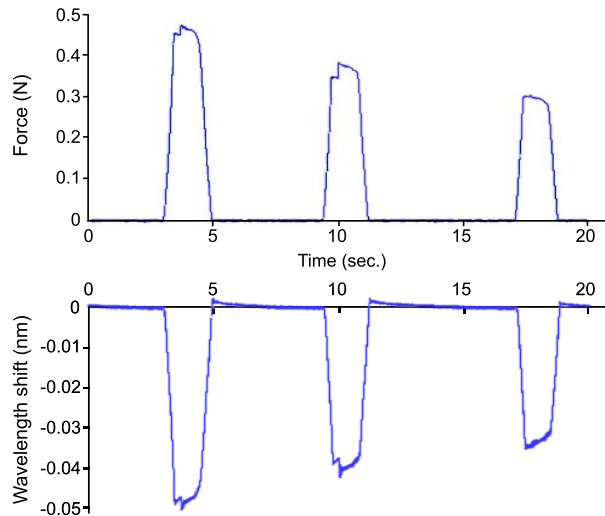


Fig. 8. Axial tip force measured by the load cell (top) and the reflection wavelength shift of the FBG in the tip measured by the optical interrogator (bottom) without actuation of the linear motor.

deformation is linear for the desired range of applied forces, and if the fiber reading is adequate to estimate the applied force. The result also confirmed that the tip design with holes amplified the axial strain by more than 50% along the groove, as shown in Fig. 7. The optical fibers were interfaced to a dynamic optical interrogator (SM-130, Micron Optics). Tests were run while applying and measuring forces to the tip with a motorized test stand (ESM301, Mark-10) and comparing these readings to the interrogator output. Although not directly shown, all fiber readings account for temperature offsets.

1) *Without Actuation*: Multiple loading and unloading forces were applied to the tip and force measurements from a commercial load cell (STL-25, AmCells) and wavelength shifts from the FBG were recorded (Fig. 8). The readings from the optical fiber and the load cell match up, indicating that there is no time delay in this system. The fiber reading was regressed to the force output (Fig. 9). The regression shows a highly linear trend, resulting in a high R^2 (R-Squared) value of 0.996.

2) *With Actuation*: Again, we first compare the output of the load cell with the fiber (Fig. 10). It can be observed that the data is noisier than the previous data, yet the readings still line up, indicating no time delay in the system. It is

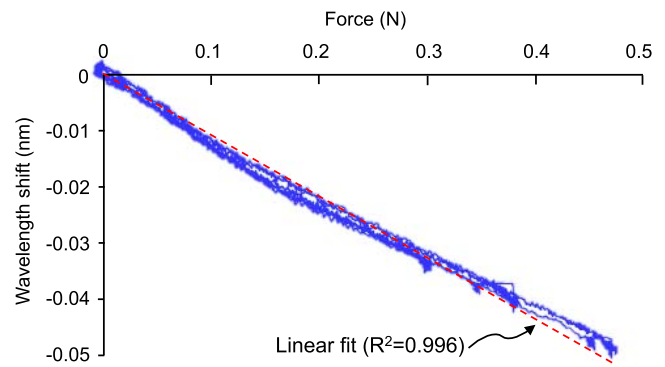


Fig. 9. Best fit line to the graph of change in wavelength versus the applied force without actuation for the data of Fig. 8.

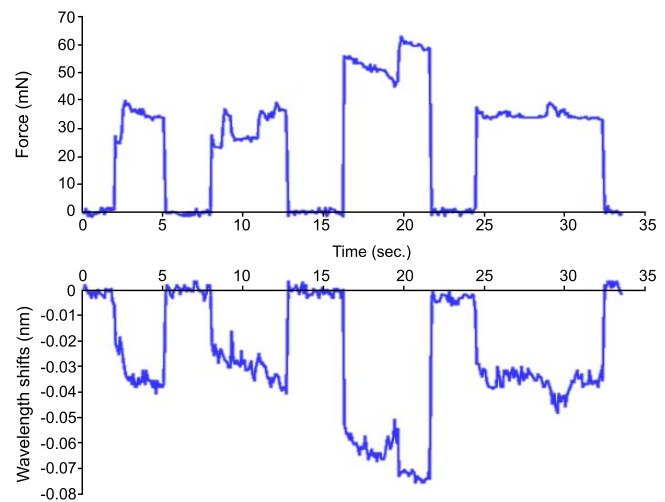


Fig. 10. Axial tip force measured by the load cell (top) and the reflection wavelength shift of the FBG in the tip measured by the optical interrogator (bottom) with actuation of the linear motor.

also observed that the force sensitivity of the FBG is much larger with actuation. This is because the spring force from the retraction spring was applied to the tip in addition to the actual tip force. We again regress the fiber reading to the load cell and find a lower R^2 of 0.951 (Fig. 11), which is to be expected, given that the data is noisier.

3) *Temperature Compensation*: FBGs are susceptible to temperature aberration, leading to offset in the measured wavelength shift. To address this issue, the actuated tip incorporates two FBGs: one that was fully glued inside the groove on the tip and the other that was partially glued to the tip. The fully glued FBG is sensitive to both temperature change and applied force while the partially glued FBG measures only the heat offset. In this way, we will be able to account for the heat offset and adjust the readings. To validate this solution, we increased the ambient temperature of the tip while gradually increasing the axial force at the same time and measured the output of each of the FBGs. The tip was placed in the open-top box to slow the spontaneous temperature change. The temperature of the tip was measured with a thermometer placed adjacent to the tip. The ambient temperature around the tip was gradually increased using a heat gun. The wavelength readings from the interrogator were recorded from 25 °C to 40 °C in increments

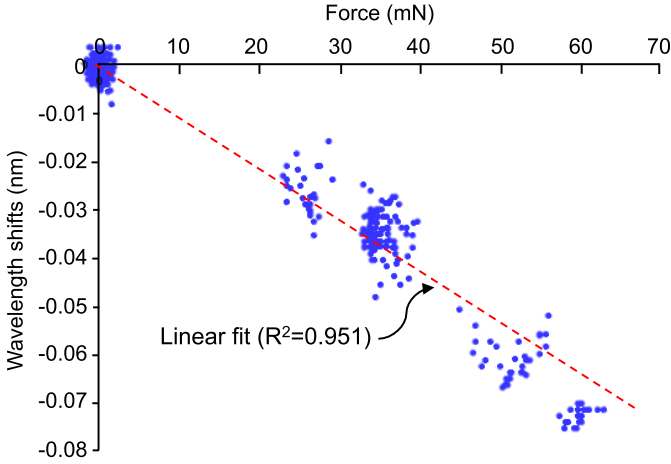


Fig. 11. Best-fit line to the graph of change in wavelength versus the applied force with actuation. The R^2 value is 0.9513, indicating a good coupling of the applied force and the reading from the optical fibers.

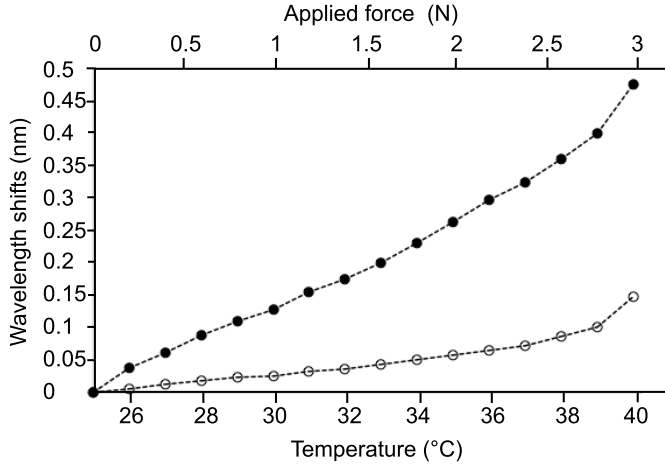


Fig. 12. Temperature recordings of the thermometer versus wavelength shift of the two optical fiber recordings from the interrogator.

of 1 °C (Fig. 12). Assuming the two fibers experience the same temperature changes, the actual force applied to the tip can be found by subtracting the outputs of the temperature compensation FBG from those of the force sensing FBG.

IV. CONTROL STRATEGY

The objective of our closed-loop controller is to control the contact force between the tip of the end-effector and the heart wall by adjusting the speed of the piezoelectric motor based on the force error $f_e = f_d - f_m$, where f_d and f_m are the desired contact force and the measured contact force from the integrated force sensor, respectively, expressed as functions of time. A simple proportional-integral-derivative (PID) controller (Fig. 13-top) can be implemented for controlling the contact force. The parameters of the PID controller will have to be determined and tuned experimentally. The goal here is rather maintaining the contact force within the safety range than precisely tracking a force setpoint, since safety is of utmost importance in the application at hand. In our system, the tip force is controlled by the speed of the piezo-motor, and the speed is controlled by the duty cycle u . Therefore, u becomes the input to the system.

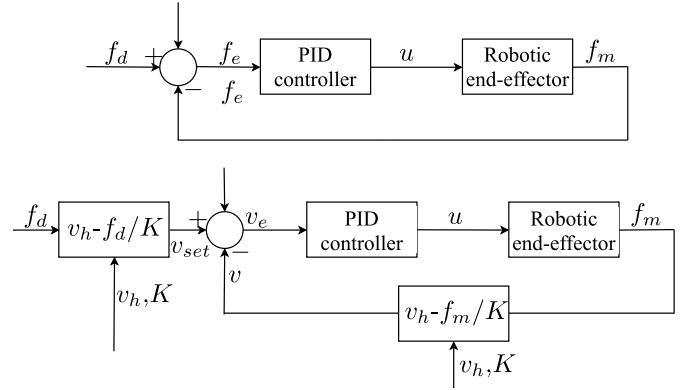


Fig. 13. Block-diagrams for closed-loop contact force control based on PID controller.

The conversion of f_e to u can also be done by modeling the contact forces as the impulse forces. Let v_h and v_t be the speeds of the heart wall and the tip, respectively. Then, the desired contact force can be expressed as $f_d = (v_h - v_{set}) \times K$, where v_{set} is the reference speed of the tip, and K is a coefficient determined experimentally. Similarly, the measured contact force can be expressed as $f_m = (v_h - v) \times K$, where v is the actual speed of the tip. The error f_e can be expressed as $f_e = (v_{set} - v) \times K$. To determine v_{set} , the speed of the heart motion, v_h needs to be given as an input. By converting the contact force to the tip speed using impulse dynamics, we use the error $v_e = v_{set} - v$ and the PID controller to generate the control input u for the piezo-motor. Therefore, we suggest two different controllers for the tracking of the contact force between the tip and the heart wall, as shown in Fig. 13.

V. DISCUSSION

In this paper, integration of actuation and sensing into the design of a miniaturized tip for catheter ablations was achieved. Experimental characterization of the actuation and sensing components individually and within the integrated setup validated the design on the basis of requirement specifications derived from the specific case of AF treatment. Design, fabrication and integration of the required actuation and sensing into a tip of cross-section less than $5 \times 5 \text{ mm}^2$ was the most challenging aspect of the current investigation and was accomplished successfully. Even though the current tip design was based on the specifications for the AF treatment, the same design and setup could be used for various other MIS procedures where catheter ablations are required or where successful treatment depends on the accurate application of the forces by the tip.

The next steps are to develop both a physical model of the procedure environment with dynamic physiological changes that would be encountered during the procedure, and a corresponding control system based on the feedback from the integrated sensor and controls tip movement to ensure delivery of the desired force to the heart wall using the actuation.

Although the robotic tip unit was designed for control of the contact force, it will not be effective if the unit is not grounded to the heart wall due to the cardiac impulse. Therefore, another area of future work is to develop an anchoring mechanism of

the tip unit. We conceive two potential mechanisms: suction anchors and a balloon anchor. Once the catheter reaches the target area, multiple suction lines hidden in the sheath are deployed and adhere to the heart wall around the target area, using vacuum created at the base of the catheter. The suction cups do not physically penetrate the surface of the heart wall, and the vacuum pressure will be controlled so that they will not cause any damage to the endocardium. Suction mechanisms for attaching a miniature device to the heart wall have previously been demonstrated in [29] and [30]. To reinforce the suction anchors, an additional mechanism, a balloon anchor, can be added. A specific part of the catheter body expands and holds a certain area of a blood vessel, such as the inferior vena cava (IVC) or ascending aorta that is often used as a passage for an ablation catheter [31].

VI. CONCLUSION

A novel miniaturized robotic end-effector that integrates a piezoelectric actuator and a fiber optic sensor was designed and prototyped for use in minimally invasive procedures, such as radiofrequency ablation of cardiac arrhythmia.

In the proposed system, the piezoelectric actuator generates bi-directional linear motions for applying and releasing axial force to a contact surface, and the optical fiber Bragg sensor embedded in the tip of the end-effector detects the axial force during actuation. The characterization result demonstrated that the end-effector was able to generate the tip force over 0.5 N at close to the target surface, and the fiber optic sensor was able to measure the axial force smaller than 25 mN.

With further optimization of the tip design and sensor placement, a higher sensitivity and accuracy should be possible in the future. Furthermore, while the current work has focused on single-axis force sensing using a single FBG, it is possible to integrate multiple FBGs in the tip for 3-axis force or deflection sensing maintain almost the same form factor.

REFERENCES

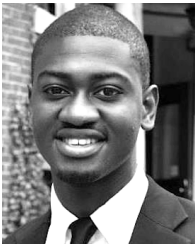
- [1] A. Pazouki, "Minimally invasive surgical sciences: A new scientific opportunity for all scientists," *J. Minimally Invasive Surg. Sci.*, vol. 1, no. 1, pp. 9–10, 2012.
- [2] F. L. Hammond, K. Shimada, and M. A. Zenati, "Measurement and optimization of minimally invasive intervention device design fitness using a multiobjective weighted isotropy index," *J. Med. Devices*, vol. 4, no. 11, pp. 011002-1–011002-9, 2010.
- [3] T. N. Robinson and G. V. Stiegmann, "Minimally invasive surgery," *Endoscopy*, vol. 36, no. 1, pp. 48–51, 2004.
- [4] J. D. Luketich *et al.*, "Minimally invasive esophagectomy," *Ann. Surg.*, vol. 238, no. 4, pp. 486–495, 2003.
- [5] J. C. Hu *et al.*, "Comparative effectiveness of minimally invasive vs open radical prostatectomy," *J. Amer. Med. Assoc.*, vol. 302, no. 14, pp. 1557–1564, 2009.
- [6] A. Dooley and G. Asimakopoulos, "Does a minimally invasive approach result in better pulmonary function postoperatively when compared with median sternotomy for coronary artery bypass graft?" *Interact. Cardiovascular Thoracic Surg.*, vol. 16, no. 6, pp. 880–885, 2013.
- [7] K. Yoshida and K. Aonuma, "Catheter ablation of atrial fibrillation: Past, present, and future directions," *J. Arrhythmia*, vol. 28, no. 2, pp. 83–90, 2012.
- [8] U. Seibold, B. Kubler, and G. Hirzinger, "Prototype of instrument for minimally invasive surgery with 6-axis force sensing capability," in *Proc. IEEE Int. Conf. Robot. Autom.*, Apr. 2005, pp. 498–503.
- [9] D. E. Haines, "Determinants of lesion size during radiofrequency catheter ablation: The role of electrode-tissue contact pressure and duration of energy delivery," *J. Cardiovascular Electrophysiol.*, vol. 2, no. 6, pp. 509–515, 1991.
- [10] R. Müller *et al.*, "Application of CVD-diamond for catheter ablation in the heart," *Diamond Relat. Mater.*, vol. 13, nos. 4–8, pp. 1080–1083, 2004.
- [11] O. J. Eick and D. Bierbaum, "Tissue temperature-controlled radiofrequency ablation," *Pacing Clin. Electrophysiol.*, vol. 26, no. 3, pp. 725–730, 2003.
- [12] C. Weiss, M. Antz, O. Eick, K. Eshagzai, T. Meinertz, and S. Willems, "Radiofrequency catheter ablation using cooled electrodes: Impact of irrigation flow rate and catheter contact pressure on lesion dimensions," *Pacing Clin. Electrophysiol.*, vol. 25, no. 4, pp. 463–469, 2002.
- [13] R. Cappato *et al.*, "Worldwide survey on the methods, efficacy, and safety of catheter ablation for human atrial fibrillation," *Circulation*, vol. 111, no. 9, pp. 1100–1105, 2005.
- [14] D. C. Shah, G. Leo, N. Aeiby, P. Gentil-Baron, H. Burri, and H. Sunthorn, "Evaluation of a new catheter sensor for real-time measurement of tissue contact," *Heart Rhythm Soc.*, vol. 3, no. 5, pp. S75–S76, 2006.
- [15] K. Yokoyama *et al.*, "Novel contact force sensor incorporated in irrigated radiofrequency ablation catheter predicts lesion size and incidence of steam pop and thrombus," *Circulation Arrhythmia Electrophysiol.*, vol. 1, no. 5, pp. 354–362, 2008.
- [16] B. Schmidt *et al.*, "Toccatà multi-center clinical study using irrigated ablation catheter with integrated contact force sensor: First results," *Heart Rhythm Soc.*, vol. 6, no. 5, p. s336, May 2009.
- [17] P. Polygerinos, L. D. Seneviratne, R. Razavi, T. Schaeffter, and K. Althoefer, "Triaxial catheter-tip force sensor for MRI-guided cardiac procedures," *IEEE/ASME Trans. Mechatronics*, vol. 18, no. 1, pp. 386–396, Feb. 2013.
- [18] P. Puangmali, K. Althoefer, L. D. Seneviratne, D. Murphy, and P. Dasgupta, "State-of-the-art in force and tactile sensing for minimally invasive surgery," *IEEE Sensors J.*, vol. 8, no. 4, pp. 371–381, Apr. 2008.
- [19] S. B. Kesner and R. D. Howe, "Force control of flexible catheter robots for beating heart surgery," in *Proc. IEEE Int. Conf. Robot. Autom.*, May 2011, pp. 1589–1594.
- [20] D. Gelman, A. C. Skanes, M. A. Tavallaci, and M. Drangova, "Design and evaluation of a catheter contact-force controller for cardiac ablation therapy," *IEEE Trans. Biomed. Eng.*, vol. 63, no. 11, pp. 2301–2307, Nov. 2016.
- [21] D. A. Henderson, "Novel piezo motor enables positive displacement microfluidic pump," in *Proc. NISTI Nanotech.*, Santa Clara, CA, USA, May 2007, pp. 1–4.
- [22] S. Yang, R. A. MacLachlan, and C. N. Riviere, "Manipulator design and operation of a six-degree-of-freedom handheld tremor-canceling microsurgical instrument," *IEEE/ASME Trans. Mechatronics*, vol. 20, no. 2, pp. 761–772, Apr. 2015.
- [23] P. Puangmali, H. Liu, L. D. Seneviratne, P. Dasgupta, and K. Althoefer, "Miniature 3-axis distal force sensor for minimally invasive surgical palpation," *IEEE/ASME Trans. Mechatronics*, vol. 17, no. 4, pp. 646–656, Aug. 2012.
- [24] Y.-L. Park, S. C. Ryu, R. J. Black, K. K. Chau, B. Moselehi, and M. R. Cutkosky, "Exoskeletal force-sensing end-effectors with embedded optical fiber-Bragg-grating sensors," *IEEE Trans. Robot.*, vol. 25, no. 6, pp. 1319–1331, Dec. 2009.
- [25] X. He, J. Handa, P. Gehlbach, R. Taylor, and I. Iordachita, "A sub-millimeter 3-DOF force sensing instrument with integrated fiber Bragg grating for retinal microsurgery," *IEEE Trans. Biomed. Eng.*, vol. 61, no. 2, pp. 522–534, Feb. 2014.
- [26] H. Moon *et al.*, "FBG-based polymer-molded shape sensor integrated with minimally invasive surgical robots," in *Proc. IEEE Int. Conf. Robot. Autom.*, May 2015, pp. 1770–1775.
- [27] Y.-L. Park *et al.*, "Real-time estimation of 3-D needle shape and deflection for MRI-guided interventions," *IEEE/ASME Trans. Mechatronics*, vol. 15, no. 6, pp. 906–915, Dec. 2009.
- [28] G. Shechter, J. R. Resar, and E. R. Mcveigh, "Displacement and velocity of the coronary arteries: Cardiac and respiratory motion," *IEEE Trans. Med. Imag.*, vol. 25, no. 3, pp. 369–375, Mar. 2006.
- [29] N. A. Patronik, T. Ota, M. A. Zenati, and C. N. Riviere, "A miniature mobile robot for navigation and positioning on the beating heart," *IEEE Trans. Robot.*, vol. 25, no. 5, pp. 1109–1124, Oct. 2009.
- [30] T. Ota, N. Patronik, D. Schwartzman, C. Riviere, and M. A. Zenati, "Subxiphoid epicardial pacing lead implantation using a miniature crawling robotic device," *J. Surg. Res.*, vol. 137, no. 2, pp. 242–243, 2007.
- [31] Y. Kanjwal, J. M. John, and M. W. Burket, "Passing sheaths and electrode catheters through inferior vena cava filters: Safer than we think?" *Catheterization Cardiovascular Intervent.*, vol. 74, no. 6, pp. 966–969, 2008.



Edgar Aranda-Michel received the B.S. degree in biomedical engineering from the Massachusetts Institute of Technology, Cambridge, MA, USA, 2014. He is currently a Medical Scientist Trainee with the University of Pittsburgh and Carnegie Mellon University, Pittsburgh, PA, USA. His research interests include biomedical robotics and cardiac assist devices.



Jaehyun Yi received the B.S. degree in mechanical engineering from the Georgia Institute of Technology, Atlanta, GA, USA, in 2015. He is currently pursuing the Ph.D. degree with the Department of Mechanical Engineering, Seoul National University, Seoul, South Korea. His research interests include design and fabrication of soft sensors and actuators.



Jackson Wirekoh received the B.S. and Ph.D. degrees in mechanical engineering from Massachusetts Institute of Technology, MA, USA, in 2013, and from Carnegie Mellon University, Pittsburgh, PA, USA, in 2017, respectively. He is currently a Research Scientist with the Orthopedics Division, NYU Langone Health, New York City, NY, USA. His research interests include soft robotics, wearable robotics, and assistive and rehabilitative devices.



Nitish Kumar received the Ph.D. degree in robotics from the University of Strasbourg, Strasbourg, France, in 2014. He is currently a Post-Doctoral Researcher with the Department of Computer Science, ETH Zurich, Switzerland. His research interests include dynamic analysis of robots and model-based robot control.



Cameron N. Riviere (S'94–M'96–SM'10) received the Ph.D. degree in mechanical engineering from Johns Hopkins University, Baltimore, MD, USA, in 1995. He is currently a Research Professor with the Robotics Institute, Carnegie Mellon University, Pittsburgh, PA, USA. His research interests include medical robotics, control systems, signal processing, and human-machine interfaces. He is an Associate Editor on the Conference Editorial Boards of the IEEE Robotics and Automation Society and the IEEE Engineering Medicine and Biology Society.



David S. Schwartzman received the medical degree from New York University in 1985, where he completed his internship and residency. With over 25 years of clinical and research experience, he specializes in the electricity of the heart and its rhythm. He is currently a Cardiac Electrophysiologist with Butler Health Systems, Butler, PA, USA. He is a Fellow of the American College of Cardiology, the American Heart Association, and the Heart Rhythm Society.



Yong-Lae Park (M'10) received the Ph.D. degree in mechanical engineering from Stanford University, Stanford, CA, USA, in 2010. He was an Assistant Professor with the Robotics Institute, Carnegie Mellon University, Pittsburgh, PA, USA, from 2013 to 2017, and a Technology Development Fellow with the Wyss Institute of Biologically Inspired Engineering, Harvard University, Cambridge, MA, USA, from 2010 to 2013. He is currently an Associate Professor with the Department of Mechanical Engineering, Seoul National University, Seoul, South Korea. His research interests include soft robotics, bio-inspired robotics, and wearable robotics.